IJARSCT
International Journal of Advanced Research in Science, Communication and Technology
International Open-Access, Double-Blind, Peer-Reviewed, Refereed, Multidisciplinary Online Journal
ISSN: 2581-9429
Volume 6, Issue 10, March 2026
Impact Factor: 8.2

Effect of Lead Substitution on Optical, and Electrical Properties of Cobalt Nanoferrite Synthesized by Sol-Gel Method

Altaf Isuf Fakir, Mehboob Nagarbawdi, Iffa Ismail Karbari
Department of Physics, Anjuman Islam Janjira Degree College of Science, Murud-Janjira, Raigad, Maharashtra, India
Arham International Institute of Information Security, Pune
Affiliated to Savitribai Phule Pune University Pune, India

Abstract: *Lead doped (Pb^{2+}) cobalt (Co) Nanoferrite as Co1-xPbxFe2O4 (were x=0.1,0.2,0.3,0.4,0.5) were synthesized by a simple cost-effective method involving sol-gel auto combustion method. Synthesized samples were sintered at 600°C temperature. The powders resulting from this synthesis were characterized by X-ray diffraction (XRD). The grain size was found to be in the range of 34.5-54.5 nm. It was found that grain size first increases up to x = 0.3 and then decreases for higher Pb2+ substitution. The absence of any extra peak in diffraction pattern ensures the phase purity for all samples. All the peaks are well matched with standard JCPDS data for CoFe2O4 (22-1086). It was also found that lattice parameter is in the range from 8.3877 Å to 8.4108 Å. From UV-Vis absorbance spectra it was found that an absorption edge of all sample appears in the range of 690 nm to 703 nm. It is seen that with increasing dopant concentration of Pb2+ band gap first decreases up to concentration x=0.3 then increases up to x=0.5. from AC conductivity result it is seen that AC conductivity increases linearly with the frequency, due to electron hopping between Pb2+ and Fe3+ ions on the octahedral sites. It is also evident that the frequency dependent ac electrical conductivity of Co1-xPbxFe2O4 are remarkably dependent on the lead content in the ceramics. The conductivity decrease with increasing lead concentration.*

Keywords: Sol-gel; Pb-Co nanoferrite; XRD; UV; AC Conductivity etc.

I. INTRODUCTION

Cobalt ferrites have garnered significant interest due to their wide range of industrial and research applications, attributed to their excellent magnetic, electrical, and structural properties. Among the ferrite group. Additionally, the replacement of different cations in cobalt ferrites, such as Zn^{2+}, Ni^{2+}, Cu^{2+}, and Pb^{2+}, allows for adjustable changes in their characteristics, improving their functionality for a range of applications [1]. High-frequency gadgets, memory cores, high-density data storage, and biological uses including ferrofluids, magnetic drug delivery, and cancer treatment hyperthermia are a few examples [2]. $CoFe_2O_4$ has an inverse spinel structure in which Co^{2+} ions are in octahedral (B) position while Fe^{3+} ions are in tetrahedral (A) and octahedral (B) positions. Pb^{2+} substitution in $CoFe_2O_4$ may result in distorted spinel structures depending on the concentration of precursor solutions, since PbFe2O4 exhibits a typical spinel structure with Pb^{2+} ions in tetrahedral sites and Fe^{3+} ions in octahedral sites. The sol-gel approach is unique among synthesis procedures since it can quickly and at relatively low temperatures generate ultrafine ferrite powders with remarkable compositional uniformity [3]. It has been observed that The DC electrical resistivity of the samples increased with higher Pb^{2+} concentration from x=0.1 to x=0.5, indicating decreased conductivity, though it improved with increasing voltage [4]. In order to investigate the impact of Pb^{2+} ion concentration on the material's structural, optical and electrical properties, this work uses the sol-gel method to synthesise Lead substituted cobalt ferrite nanoparticles ($Co_{1-x}Pb_xFe_2O_4$, where x = 0.1-0.5).

DOI: 10.48175/IJARSCT-35006

IJARSCT
International Journal of Advanced Research in Science, Communication and Technology
International Open-Access, Double-Blind, Peer-Reviewed, Refereed, Multidisciplinary Online Journal
ISSN: 2581-9429 Volume 6, Issue 10, March 2026 Impact Factor: 8.2

In this work, lead (Pb^{2+}) substituted cobalt ferrite ($Co_xPb_{1-x}Fe_2O_4$) nanoparticles are synthesised using the sol-gel method, and the impact of Pb^{2+} ion concentration on the optical and electric properties of the Co-ferrite nanoparticles is studied.

II. EXPERIMENTAL

2.1 Materials

Analytical grade nitrate, such as cobalt nitrate ($Co(No_3)_2.6H_2o$), lead nitrate ($Pb(No_3)_2$), ferric nitrate ($Fe_2(No_3)_2$) and citric acid ($C_6H_8O_7$) which are used as fuel in a 1:3 ratios and are supplied by Merck with approximately 99 percent purity, were used as starting materials for the synthesis without additional purification.

Chemicals	Molecular Formula	Molecular Weight
cobalt nitrate	$Co(No_3)_2.6H_2O$	291.03
lead nitrate	$Pb\ (No_3)_2$	331.20
ferric nitrate	$Fe(NO_3)_3 9H_2O$	404.00
Citric Acid	$C_6H_8O_7$	192.13

2.2 Chemical reaction:

$$Co(No_3)_2.6H_2O + Pb\ (No_3)_2 + Fe(NO_3)_3.9H_2O + 3C_6H_8O_7 \xrightarrow{100^0C \text{ for } 4h} CoPbFe_2O_4$$

Synthesis Procedure:

Sol-gel synthesis method was performed to create Pb^{2+}substituted $CoFe_2O_4$ ferrite, which has the chemical formula $Co_{1-x}Pb_xFe_2O_4$ (where x = 0.1, 0.2, 0.3, 0.4, and 0.5). As Illustrated in figure 1 under magnetic stirring, 100 ml of distilled water were used to dissolve the stoichiometric amounts of ferric nitrate ($Fe(NO_3)_2$), lead nitrate ($Pb\ (No_3)_2$), and cobalt nitrate $Co(No_3)_2.6H_2O$. The metal nitrate solution was then combined with citric acid ($C_6H_8O_7$) to remove the Co^{2+}, Pb^{2+}, and Fe^{2+} ions. A molar ratio of 1:3 was maintained between citric acid and total moles of nitrates. To maintain the stability of the nitrate-citrate solution and bring the pH down to roughly 7, a small quantity of ammonia was added to the mixture drop by drop. After vigorous stirring and an hour of heating at 100°C, the solution was allowed to evaporate and was maintained at this temperature until it solidified into a gel. After that, the gel was heated to 150°C to begin auto-combustion. The resultant powder is crushed in an agate mortar and sintered for four hours at 600 °C to produce the nanoferrite particles.

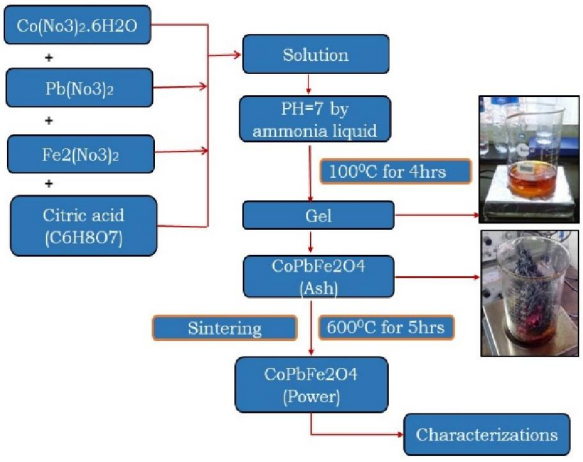

Figure 1 Synthesis process of Pb^{2+}substituted $CoFe_2O_4$ ferrite

IJARSCT
International Journal of Advanced Research in Science, Communication and Technology
International Open-Access, Double-Blind, Peer-Reviewed, Refereed, Multidisciplinary Online Journal
ISSN: 2581-9429 Volume 6, Issue 10, March 2026 Impact Factor: 8.2

2.4 Characterization Techniques:Pb^{2+}substituted $CoFe_2O_4$ ferrites have been found structurally and subjected to phase investigation using XRD patterns. Cu-Kα radiation (λ = 1.54182 Å) was used to record the pattern in the 2θ range of 20° to 80° with a step size of 0.01° and time/step of 2s. Dielectrical properties of $Co_{1-x}Pb_xFe_2O_4$ (x = 0.1, 0.2, 0.3, 0.4 and 0.5) were studied at room temperature using multi frequency LCR-Q meter.The powders samples were mixed with polyvinyl alcohol (PVA) agent as a binder and pressed into cylindrical pellets with 9-mm diameter and 3-mm thickness under the pressure of 5 tons. The pellets were sintered in a muffle furnace at 200 °C for 2 h for removal of binder and used for bulk density, electrical and di electrical measurements.To ensure good Ohmic contact, the pellets were coated with silver paste and polished for smooth parallel faces.The dielectric properties of all the samples were measured using the LCR-Q meter as a function of frequencies in the range 50 Hz - 5 MHz at room temperature. The dielectric constant (ε') was calculated using the formula,

$$\varepsilon' = \frac{Cd}{\varepsilon o A}$$

where A represents the cross-sectional area of the flat surface of the pellet, C represents its capacitance in farad, d represents its thickness in meters and εo is the constant of permittivity for free space.The energy loss is generally characterized by the dielectric loss factor (tanδ) and expressed as,

$$\tan\delta = \varepsilon'' / \varepsilon'$$

where the phase difference between the induced current and the applied electric field is represented by the angle δ. where ε' is the dielectric constant's real portion and ε" is its imaginary part, which indicates how much energy the dielectric absorbs from the alternating field. Dielectric losses arise if the polarization lags behind the applied alternating field which may be caused by grain boundaries, impurities and imperfections in the crystal [5]. The AC conductivity (σ_{ac}) of all sample measured at room temperature with frequency in the range 50Hz to 5MHz. The a.c. conductivity obtained from following equation,

$$\sigma_{ac} = \varepsilon' \varepsilon_o \omega \tan\delta$$

Where ω = 2πf and is the angular frequency,ε_o is permittivity of free space and tan δ is the dielectric loss tangent.

III. RESULTS AND DISCUSSION

3.1 X-Ray Diffraction: Fig. 2 (a) displays the XRD patterns for the Pb-doped $CoFe_2O_4$ samples at x = 0.1, 0.2, 0.3, 0.4, and 0.5. The average grain size (t) was calculated using the Debye-Scherrer formula, which yielded values between 34.5 and 54.5 nm in the present investigation. Observations made on the increase of the Pb^{2+} level showed the estimated particle size to be very arbitrary, even when regenerated under the same conditions [6]. Lack of Additional peaks in Diffraction patterns guarantee phase purity of samples. All peaks presented good matches to the JCPDS data files (JCPDS No. 22-1086) for $CoFe_2O_4$, the lattice parameter (a) was calculated using the formula above.

$$a = d \times \sqrt{h^2 + k^2 + l^2}$$

The index "*hkl*" refers to the X-ray diffraction reflection peak and "*d*" refers to the interplanar distance. As the computation of the "a" lattice parameter of a particular reflex peak from the XRD pattern has helped to make the lattice constant known with certainty, it is always the average value of the peaks. Whereas the lattice parameters are in the range 8.3877 to 8.4108 Å. The increase in the lattice parameter with higher Pb^{2+} content could be understood on the basis of ionic radii: The Pb^{2+} ion (1.19 Å) being somewhat larger in size than the Co^{2+} ion (0.7 Å), causing lattice expansion. The shift of the diffraction angle 2θ, due to the increasing content of Pb^{2+}, is illustrated in Figure 2(b). In this study, it is found that a peak at a lower angle shifts in x = 0.3, 0.4, 0.5 with respect to x = 0.1 and a peak at a higher angle shifts in x = 0.2. Lower angle shifts in peak suggest that there is compressive strain and the interplanar spacing (d) is of an increasing value; while higher angle shifts in peak suggest that there is tensile strain and the interplanar spacing (d) is of a decreasing value.

IJARSCT
International Journal of Advanced Research in Science, Communication and Technology
International Open-Access, Double-Blind, Peer-Reviewed, Refereed, Multidisciplinary Online Journal
ISSN: 2581-9429
Volume 6, Issue 10, March 2026
Impact Factor: 8.2

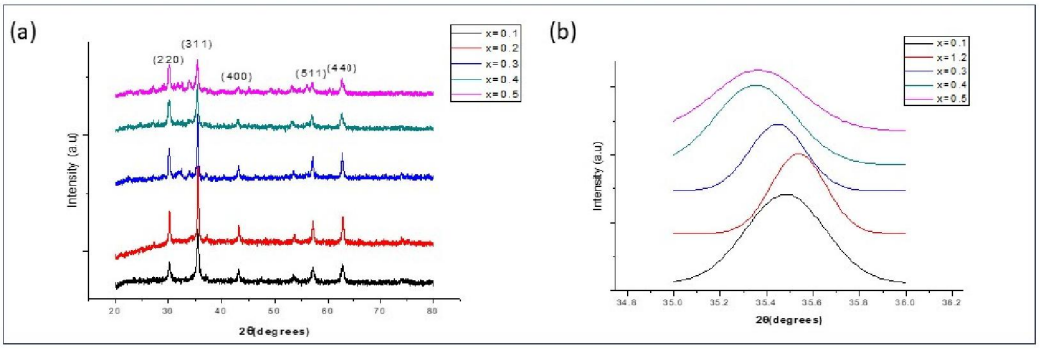

Figure 2 (a)XRD patterns for the Pb^{2+} substituted $CoFe_2O_4$ samples with the Pb^{2+} concentration of x = 0.1, 0.2, 0.3,0.4,0.5.(b) Graph of Diffraction angle 2θ shift with increase in Pb^{2+} concentration.

3.2 UV-Visible spectroscopyUV-Visible spectroscopy is ideal for characterizing optical and electronic properties of many different materials. In many studies, the energy gap (Eg) is an important feature of semiconductors which determines their applications in optoelectronics. Figure 3 shows the UV–Vis absorbance spectra of the Pb^{2+} doped $CoFe_2O_4$ with x=0.1,0.2,0.3,0.4,0.5 recorded at room temperature. An absorption edge of all sample appears in the range of 690nm to 703nm.using the absorption edge one can determine the energy gap (E=hc/λ). where h is planck constant (h = 4.13566×10^{-15}), c is velocity of light and λ is wavelength of absorption edge. By using above relation obtained band gap for all the ferrites is listed in Table 1.

Table 1

Sr No.	composition	Absorption Wavelength (λ) nm	Band gap (ev)
1	$Co_{0.9}Pb_{0.1}Fe_2O_4$	696.5	1.7803
2	$Co_{0.8}Pb_{0.2}Fe_2O_4$	697.5	1.7776
3	$Co_{0.7}Pb_{0.3}Fe_2O_4$	703.63	1.7622
4	$Co_{0.6}Pb_{0.4}Fe_2O_4$	700.45	1.7702
5	$Co_{0.5}Pb_{0.5}Fe_2O_4$	696.46	1.7804

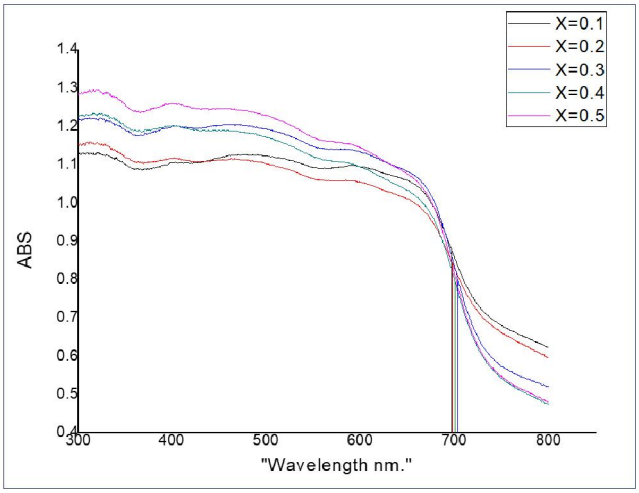

Figure 3 UV absorption spectra Pb^{2+} doped $CoFe_2O_4$ with x=0.1,0.2,0.3,0.4,0.5 (recorded at room temperature).

DOI: 10.48175/IJARSCT-35006

IJARSCT
International Journal of Advanced Research in Science, Communication and Technology
International Open-Access, Double-Blind, Peer-Reviewed, Refereed, Multidisciplinary Online Journal
ISSN: 2581-9429 Volume 6, Issue 10, March 2026 Impact Factor: 8.2

Figure 4shows Tauc plot for Pb^{2+} doped $CoFe_2O_4$ with x=0.1, 0.2, 0.3, 0.4, 0.5. The optical band gap obtained by Tauc relation of all composition is found to be nearly same as obtained by relation E=hc/λ. It is seen that with increasing dopant concentration of Pb^{2+} band gap first decreases up to concentration x=0.3 then increases up to x=0.5 as shown in Figure 5. As Pb^{2+} replaces Co^{2+}, impurity bands are created due to the formation of the impurity levels inside the gap. At low Pb^{2+} dopant concentration, the distances between the valence band and the lowest impurity band act like effective band gaps. With increasing Pb^{2+} dopant content, the widths of these impurity bands increases and these bands could overlap together leads to decrease in energy band gap (E_g) [7].The optical energy band gap goes on decreasing with increasing Pb^{2+} concentration up to x=0.3 it may be due to increase in grain size with increasing Pb^{2+} (x=0.3) concentration. Bands are genuinely created in bulk matter by the convergence of numerous neighbouring energy levels of atoms and molecules. As the particle size reaches the nanoscale, where every particle is made up of very small number of atoms or molecules, the number of overlapping of orbitals or energy level decreases and the width of the band gets narrower, this will increase band gap, hence band gap decreases with increasing grain size. On further increase in doping of Pb^{2+} (x>0.3) band gap increases which may be due to Burstein-Moss effect [8]. The phenomenon known as the Burstein-Moss effect occurs when all states near the conduction band are populated, pushing the absorption edge to higher energies and increasing the apparent band gap of a semiconductor. As the doping concentration is increased, electrons populate states within the conduction band which pushes the Fermi level higher in energy level and the Fermi level lies inside the conduction band. Since all the states below the Fermi level are occupied states, thus we observe an increase in the apparent band gap. Apparent band gap is equal to Actual band gap plus Burstein Moss shift. It may be due to decrease in grain size with increasing Pb^{2+} (x > 0.3) concentration and as grain size decreases band gap increases [9]. Our results of UV-Vis absorption study well matched with the XRD results. The change in band gap with Pb^{2+} concentration is shown in Figure 4.5.

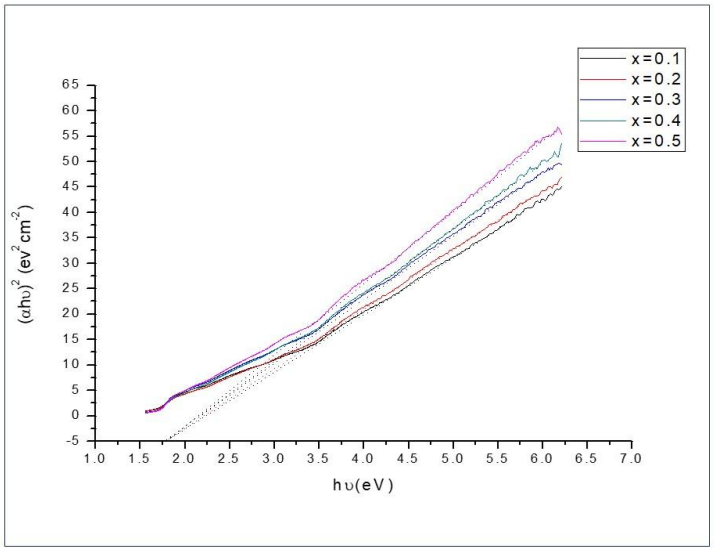

Figure 4 Tauc plot for Pb^{2+} doped $CoFe_2O_4$ with x=0.1, 0.2, 0.3, 0.4, 0.5.

IJARSCT
International Journal of Advanced Research in Science, Communication and Technology
International Open-Access, Double-Blind, Peer-Reviewed, Refereed, Multidisciplinary Online Journal
ISSN: 2581-9429
Volume 6, Issue 10, March 2026
Impact Factor: 8.2

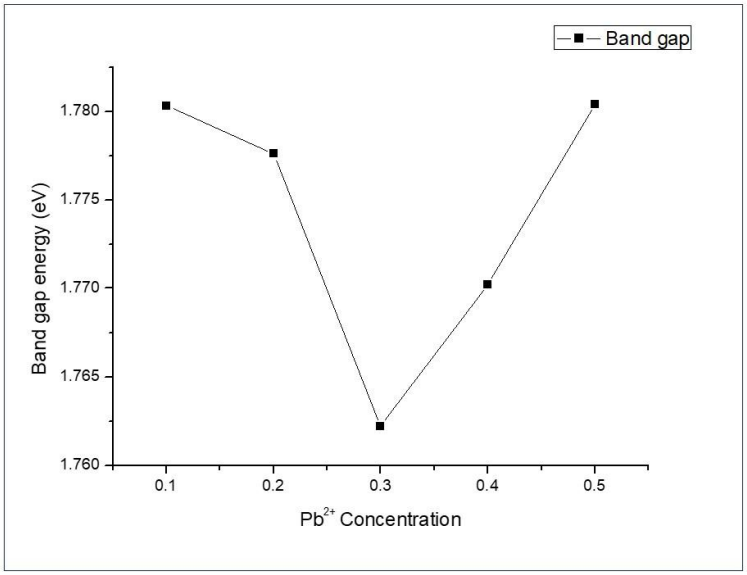

Figure 5 Change in band gap energy with Pb^{2+} concentration.

3.3 Electric properties

It is observed from Figure 6that the dielectric constant was high at low frequency may be due to dislocations, voids and defects present in the crystal structure.Dielectric constant initially decreases rapidly with increases in frequency up to a certain Frequency and beyond this frequency that remains fairly constant. It is considered that conducting grains make up ferrite samples, which are divided by non-conducting grain boundaries. When electrons reach such non conducting grain boundaries through hopping, and due to the high resistance of the grain boundaries, the electrons pile up at the grain boundaries and produce space charge polarization**.** This variation of dielectric constant depends on polarized space charge. The defects present in the crystal structure can cause a positive or negative space charge distribution in interfaces. The space charges can move under the application of an external field and when they are trapped by the defects, lots of dipole moments (space charge polarization) are formed. For low frequencies of applied field the dipole moment can easily follow the change of electric field resulting in a high value of polarization and there by a high value of dielectric constant. As frequency of the applied field increases, a point will be reached where the space charge cannot sustain with the field and hence polarization decreases [10]. The electron hopping ($Fe^{2+} \leftrightarrow Fe^{3+}$ or $Pb^{2+} \leftrightarrow Pb^{3+}$) occurs by electron transfer between adjacent octahedral sites (B-sites) in the spinel lattice [11]. Thus by the electronic exchange:

$Fe^{2+} + Pb^{3+} \longleftrightarrow Fe^{3+} + Pb^{2+}$.

One can obtain local displacements of electrons in the direction of the applied electric field. The decrease in dielectric constant with increasing Pb^{2+} content and frequency may be due to the migration of Fe^{3+} ions from octahedral site to tetrahedral site which decreases the hopping and hence decreases the Polarization [12].

DOI: 10.48175/IJARSCT-35006

IJARSCT
International Journal of Advanced Research in Science, Communication and Technology
International Open-Access, Double-Blind, Peer-Reviewed, Refereed, Multidisciplinary Online Journal
ISSN: 2581-9429
Volume 6, Issue 10, March 2026
Impact Factor: 8.2

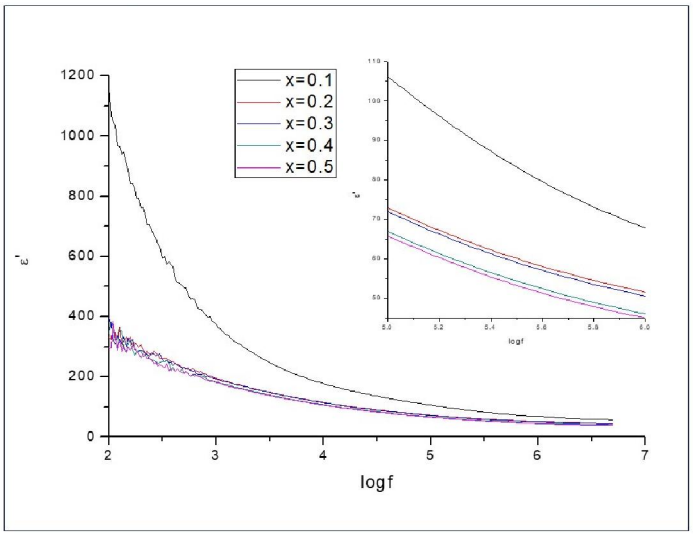

Figure 6shows the frequency dependence of the dielectric constant of the prepared samples and the inset shows partially enlarged image of the graph with different concentration curve.

The variation of AC conductivity as a function of frequency is represented in Figure 7. From figure it is seen that AC conductivity increases linearly with the frequency. The frequency dependent ac electrical conductivity of ferrites is generally accepted due to electron hopping between Pb^{2+} and Fe^{3+} ions on the octahedral sites [13]. In the present case, the observed increase in σ_{ac} with increasing frequency can be attributed to the increased hopping rate with increasing frequency. At lower frequencies the grain boundaries are more active and hence the hopping of Fe^{2+} and Fe^{3+} ions is less at lower. On increasing AC field, the conductive grains become more active thereby promoting the hopping between Fe^{2+} and Fe^{3+} ions, thereby increasing the hopping conduction [14]. It is well known that AC conductivity in disordered solids is directly proportional to frequency. It is also evident that the frequency dependent ac electrical conductivity of $Co_{1-x}Pb_xFe_2O_4$are remarkably dependent on the Pb^{2+}content in the ceramics. The conductivity decrease with increasing Pb(x).

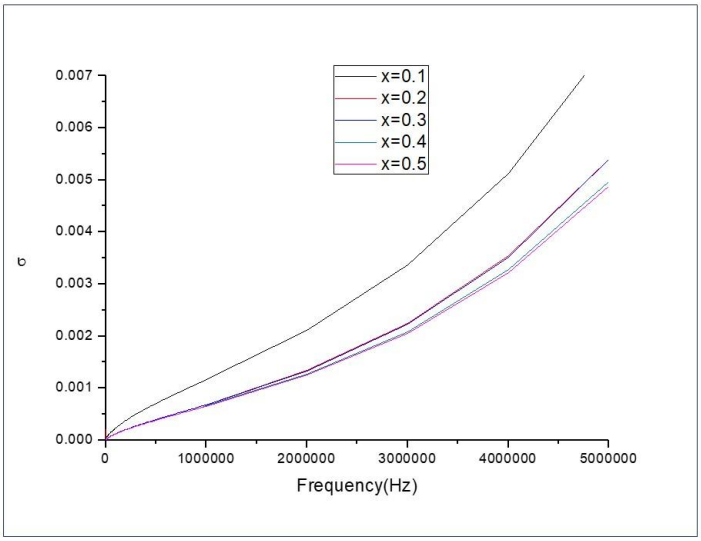

Figure 7 Variation of AC conductivity as a function of frequency.

DOI: 10.48175/IJARSCT-35006

IJARSCT
International Journal of Advanced Research in Science, Communication and Technology
International Open-Access, Double-Blind, Peer-Reviewed, Refereed, Multidisciplinary Online Journal
ISSN: 2581-9429
Volume 6, Issue 10, March 2026
Impact Factor: 8.2

IV. CONCLUSION

Lead substituted cobalt ferrite nanoparticles ($Co_{1-x}Pb_xFe_2O_4$with x = 0.1, 0.2, 0.3, 0.4, and 0.5) were prepared via sol-gel auto combustion route. From x-ray analysis, it has been found that the average crystallite size is in the range of 34.5–54.5 nm. The absence of any extra peak in diffraction pattern ensures the phase purity for all samples. All the peaks are well matched with standard JCPDS data for $CoFe_2O_4$ (22-1086). It was also found that lattice parameter is in the range from 8.3877 Å to 8.4108 Å. From UV–Vis absorbance spectra it was found that an absorption edge of all sample appears in the range of 690nm to 703nm. It is seen that with increasing dopant concentration of Pb^{2+} band gap first decreases up to concentration x=0.3 then increases up to x=0.5. from AC conductivity result it is seen that AC conductivity increases linearly with the frequency, due to electron hopping between Pb^{2+} and Fe^{3+} ions on the octahedral sites. It is also evident that the frequency dependent ac electrical conductivity of $Co_{1-x}Pb_xFe_2O_4$ are remarkably dependent on the Pb^{2+}content in the ceramics. The conductivity decrease with increasing Pb^{2+} concentration.

REFERENCES

[1] D. S. Mathew and R. S. Juang, "An overview of the structure and magnetism of spinel ferrite nanoparticles and their synthesis in microemulsions," *Chem. Eng. J.*, vol. 129, no. 1–3, pp. 51–65, May 2007, doi:10.1016/J.CEJ.2006.11.001.

[2] C. Moya, M. D. P. Morales, X. Batlle, and A. Labarta, "Tuning the magnetic properties of Co-ferrite nanoparticles through the 1,2-hexadecanediol concentration in the reaction mixture," Phys. Chem. Chem Phys., vol. 17, no. 19, pp. 13143–13149, 2015, doi: 10.1039/c5cp01052g.

[3] Shirsath, Sagar & Wang, Danyang & Jadhav, Swati & Mane, Maheshkumar & Li, Sean. (2018). Ferrites Obtained by Sol-Gel Method. 10.1007/978-3-319-32101-1_125.

[4] Altaf Isuf Fakir, Mehrab M. Hukebardar, Aditi J. More.Effect of Pb^{2+} Doping on the Electrical Properties of Cobalt Ferrite Nano Particles Prepared via Sol-Gel Route.IJARSCT,Volume 3, Issue 19, May 2023,ISSN (Online) 2581-9429.

[5] RV Mangalaraja, P Manohar, FD Gnanam, M Awano. Electrical and magnetic properties of Ni0.8Zn0.2Fe2O4/silica composite prepared by sol-gel method. Journal of materials science 39, 2037-2042.

[6] M. Lakshmi, K. V. Kumar, K. Thyagarajan, M. Lakshmi, K. V. Kumar, and K. Thyagarajan, "Structural and Magnetic Properties of Cr-Co Nanoferrite Particles," Adv. Nanoparticles, vol. 5, no. 1, pp. 103–113, Feb. 2016, doi:10.4236/ANP.2016.51012

[7] Pramanik, Md. B., al Rakib, Md. A., Siddik, Md. A., & Bhuiyan, S. (2024). Doping Effects and Relationship between Energy Band Gaps, Impact of Ionization Coefficient and Light Absorption Coefficient in Semiconductors. *European Journal of Engineering and Technology Research*, *9*(1), 10–15. https://doi.org/10.24018/EJENG.2024.9.1.3118.

[8] Zervos, M., Othonos, A., Tanasă, E., & Vasile, E. (2019). High-Temperature Pb Doping of SnO2 and Growth Limitations of PbxSn1- xO2 Nanowires Versus Low-Temperature Growth of PbxSn1- xO for Energy Storage and Conversion. *Journal of Physical Chemistry C*, *123*(26), 16415–16423. https://doi.org/10.1021/ACS.JPCC.9B02865

[9] Sun, Q. C., Yadgarov, L., Rosentsveig, R., Seifert, G., Tenne, R., & Musfeldt, J. L. (2013). Observation of a burstein-moss shift in rhenium-doped MoS2 nanoparticles. *ACS Nano*, *7*(4), 3506–3511. https://doi.org/10.1021/NN400464G

[10] Kao, K. C. (2004). Electric Polarization and Relaxation. *Dielectric Phenomena in Solids*, 41–114. https://doi.org/10.1016/B978-012396561-5/50012-8

[11] Gupta, M. P., Sinha, A. P. B., Kanetkar, S. M., Date, S. K., & Nigavekar, A. S. (1979). Evidence of electron exchange between Fe2+ and Fe3+ ions on tetrahedral and octahedral sites in Fe2MoO4. *Journal of Physics C: Solid State Physics*, *12*(12), 2401–2409. https://doi.org/10.1088/0022-3719/12/12/025

[12] Assar, S. T., El-Ghazzawy, E. H., & Abosheiasha, H. F. (2022). Study on dielectric properties, electric modulus, and impedance spectroscopy of Ni–Ca ferrite nanoparticles. *Materials Chemistry and Physics*, *287*, 126336. https://doi.org/10.1016/J.MATCHEMPHYS.2022.126336

IJARSCT
International Journal of Advanced Research in Science, Communication and Technology
International Open-Access, Double-Blind, Peer-Reviewed, Refereed, Multidisciplinary Online Journal
ISSN: 2581-9429
Volume 6, Issue 10, March 2026
Impact Factor: 8.2

[13] Bellad, S. S., & Chougule, B. K. (2000). Composition and frequency dependent dielectric properties of Li-Mg-Ti ferrites. *Materials Chemistry and Physics*, *66*(1), 58–63. https://doi.org/10.1016/S0254-0584(00)00273-X
[14] Al-Hammadi, A. H., & Khoreem, S. H. (2023). *Impact of Zinc Substitution on AC Conductivity Behaviors of Hexagonal Ba-Ni Ferrite Nanoparticle*. *13*(4), 364. https://doi.org/10.33263/BRIAC134.364